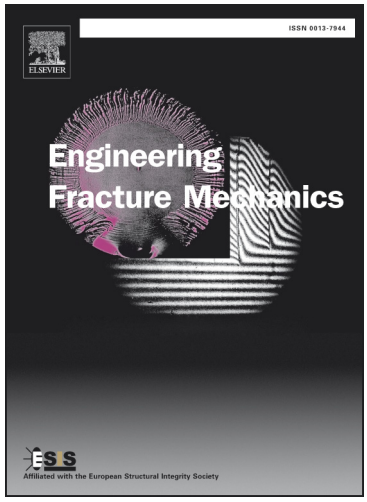

Single-specimen evaluation of tearing resistance in SENT testing

M.A. Verstraete, W. De Waele, K. Van Minnebruggen, S. Hertelé

PII: S0013-7944(15)00492-0
DOI: http://dx.doi.org/10.1016/j.engfracmech.2015.07.067
Reference: EFM 4854

To appear in: *Engineering Fracture Mechanics*

Received Date: 31 July 2014
Revised Date: 11 June 2015
Accepted Date: 24 July 2015

Please cite this article as: Verstraete, M.A., De Waele, W., Van Minnebruggen, K., Hertelé, S., Single-specimen evaluation of tearing resistance in SENT testing, *Engineering Fracture Mechanics* (2015), doi: http://dx.doi.org/10.1016/j.engfracmech.2015.07.067

Single-specimen evaluation of tearing resistance in SENT testing

M.A. Verstraete[a,*], W. De Waele[a], K. Van Minnebruggen[a], S. Hertelé[a]

[a]Laboratorium Soete, Ghent University, Faculty of Engineering and Architecture, Technologiepark gebouw 903, 9052 Zwijnaarde, Belgium
*Corresponding author: Matthias.Verstraete@UGent.be

Abstract The evaluation of CTOD tearing resistance is required by several strain based defect assessment procedures. To that extent, the use of SENT testing is widely advised as the constraint matches that of pressurized pipes. This indicates the need for well validated testing methods. This paper discusses two single specimen techniques for the evaluation of tearing resistance using clamped SENT specimens: the unloading compliance (UC) and the direct current potential drop (DCPD) technique. From the results of tests carried out on a variety of both base metal and welded specimens, both methods show a comparable accuracy and scatter.

Keywords: SENT, Unloading Compliance, Direct Current Potential Drop

1. Introduction

Several defect assessment procedures have recently been proposed to assess the criticality of pipeline girth weld defects under strain based conditions [1-2]. The majority of these procedures require the material's tearing resistance as an input. To obtain this tearing resistance, the use of Single-Edge Notched Tensile (SENT) testing is advised, given the constraint match of SENT specimens with (pressurized) pipes [3-5]. To date, the most common method for the evaluation of the tearing resistance, is the multi-specimen technique described in DNV RP-F108 [6]. Although successful applications are described in literature [7, 8], such technique involves high labor and material costs. On the other hand, the single specimen technique aims to monitor the ductile crack extension during the test. The predicted ductile crack extension can then, by means of validation, be compared to the value measured post-mortem. The latter can be obtained following the ASTM E1820 nine points average method [9].

For a successful evaluation of the tearing resistance, attention may be devoted to methods focusing on the evaluation of the crack driving force and methods focusing on the evaluation of the crack extension (Δa). For the former, both the crack tip opening displacement (CTOD) and *J*-integral can be considered to describe the crack loading. Given the equivalence between both, the CTOD parameter has arbitrarily been selected in this paper [10]. This CTOD parameter is measured using the double clip gauge method, which is well described and validated in literature for SENT testing [11, 12]. For the evaluation of the crack extension, both the unloading compliance (UC) and direct current potential drop method (DCPD) are described in literature [12-16]. It is however not clear which method yields the most accurate estimate. To that extent, this paper aims at presenting a thorough validation and comparison of both techniques for crack extension measurement. This issue was also addressed in the recently released BS8571:2014 standard for SENT testing, where reference is made to the authors' previous work in this respect [17].

Nomenclature

a	crack depth
a_0	initial crack depth
B	thickness
B_e	effective thickness

B_N	net thickness
CMOD	Crack Mouth Opening Displacement
CTOD	Crack Tip Opening Displacement
$CTOD_{ini}$	CTOD at initiation
DCPD	Direct Current Potential Drop
F_{max}	maximum force
h_1	height of first clip gauge above specimen
h_2	height of second clip gauge above specimen
H	daylight grip length
I	applied current (25 A for all tests)
MM_{FS}	mismatch in terms of flow stress
N	batch size
P_m	limit load
s_{cr}	crack front straightness parameter
SENT	Single-Edge Notched Tensile
STD	standard deviation
V	potential drop across the crack
V_1	opening of first clip gauge
V_2	opening of second clip gauge
UC	Unloading Compliance
V_{ref}	potential drop remote from the crack
W	width
WMC	Weld Metal Center
Y/T	Yield-to-Tensile ratio
δ_1	curve fitting parameter for R-curve
δ_2	curve fitting parameter for R-curve
Δa	crack extension
$\Delta a_{b,uc/pd}$	crack extension attributed to blunting for unloading compliance and potential drop method
Δa_{9p}	measured crack extension using nine points average method
δ_s	width of scatter band in terms CTOD
σ_0	yield strength
σ_{FS}	flow strength
σ_{TS}	tensile strength

2. Materials and methods

2.1. Test specimens

The SENT specimens considered in this paper have a square cross section (i.e. $B / W = 1$) and a daylight grip length (H) equal to $10W$ (Figure 1) as proposed by Shen et al. [13]. After extracting the specimens, a notch with depth a_0 is introduced through saw-cutting. The cutting blade used for the final pass is extremely sharp and thin, resulting in an initial notch root radius of 0.075 mm. Fatigue pre-cracking is not applied. This would complicate the control of the initial crack depth and is not required for sufficiently ductile materials [12,18,19].

Due to the difference in constraint at mid-thickness (towards plane strain) and at the sides (plane stress) of the specimen, crack tunneling is expected [20]. This tunneling results in a deteriorated accuracy of crack growth measurements [21]. V-shaped side grooves are machined at both sides of the test specimen to promote uniform crack extension, achieving a total thickness reduction of 15% ($B_N = 0.85W$) as advised by Shen et al. [22] side grooves are produced conform the ASTM E1820 requirements, i.e. having an opening angle less than 90° and a root radius of 0.5 ± 0.2 mm [9].

2.2. Test conditions

The specimens are clamped using hydraulic grips, restricting all rotational degrees of freedom. Following, the specimen is loaded under displacement control with a displacement rate of 0.01 mm/sec, thus representing quasi-static conditions. To allow for the evaluation of the compliances during the test, the specimens are partially unloaded and reloaded during the tests. The design of these loading cycles has been adopted from the recommended practice provided by CANMET MTL in the framework of a round robin test program [23]:

- Six unloading cycles are performed in the elastic regime when the applied force equals P_m, equal to

$$P_m = \frac{1}{2}\frac{\sigma_0 + \sigma_{TS}}{2}(W - a_0)B_e \tag{1}$$

where the effective width (B_e) is determined from the following equation:

$$B_e = B - \frac{(B - B_N)^2}{B} \tag{2}$$

The amount of unloading equals $P_m/2$.

- Following these elastic unloading cycles, subsequent unloading cycles are performed at fixed intervals of the crack mouth opening displacement (CMOD). In all cycles the amount of unloading is force controlled and also equals $P_m/2$. For the first five plastic unloading cycles the CMOD intervals equal 0.02 mm, subsequently intervals of 0.04 mm are used. The test is stopped when the applied tensile force no longer exceeds 80% of its maximum (F_{max}).

2.3. Test material

The methods presented in the remainder of this paper are applied to a series of specimens extracted from different (girth welded) pipes. To demonstrate the general applicability of the presented procedures, a broad range of testing conditions are covered, both with respect to the tested materials and geometry. More specifically, specimens with the following properties have been tested:

- Both welded and non-welded specimens have been tested, with the notch in the weld metal center (WMC) line for the welded specimens.
- The specimens are extracted from pipes with a variety of pipe grades, ranging between API-5L grades X65 and X80.
- The welded specimens are extracted from girth welds created with two different welding processes, namely shielded metal arc welding (SMAW) and gas metal arc welding (GWAW).
- The variety of welded and non-welded specimens, resulted in yield-to-tensile (Y/T) ratios between 0.82 and 0.92 for the base metal (Y/T_{BM}), and between 0.83 and 0.94 for the weld metal (Y/T_{WM}).
- The strength difference between base and weld metal, in terms of flow stress (MM_{FS}), ranges between 0% and 33%. This mismatch definition was adopted as it has shown to be connected to the tensile strain capacity for strain-based design applications [24] and defined by the following equation:

$$MM_{FS} = \frac{\sigma_{FS,WM} - \sigma_{FS,BM}}{\sigma_{FS,BM}} \quad (3)$$

- From a geometrical point, different relative crack depths have been tested. The a_0/W-ratio ranges between 0.20 and 0.60.

An overview of all tested specimens is provided in Tables 1 and 2 for the tests performed on base metal and welded specimens respectively.

2.4. CTOD measurement

A commonly applied method for the evaluation of the CTOD in SENT testing, is the double clip gauge method [25-27]. The method considered in this publication essentially relies on Rice's 90° degrees intercept method [28], starting from the original crack tip. In previous work, the authors have demonstrated the validity and equivalence of this method by comparison with the δ_5 method developed by the Helmholtz-Zentrum Geesthacht (formerly GKSS) [29]. In practice, two small mounting pieces are bolted onto the specimen's top surface, facilitating the attachment of two clip gauges on the knife-like ends (Figure 2). Therefore, two 3.0 mm deep holes with a diameter of 1.9 mm are drilled at each side of the crack. These holes are located 4.5 mm apart from the cracked ligament, resulting in an initial clip gauge opening of 3.0 mm. The height for the attachment of the clip gauges, h_1 and h_2, equals 2.0 and 8.0 mm respectively. From the change of both clip gauge readings, V_1 and V_2, the CTOD is subsequently calculated. It is thereby assumed that the crack faces do not deform plastically, but rather behave as rigid arms rotating around a point [30].

$$CTOD = 2\frac{V_2(a_0 + h_1) - V_1(a_0 + h_2)}{(V_2 - V_1) - 2(h_2 - h_1)} \quad (4)$$

In addition to the CTOD data, the double clip gauge method allows the crack mouth opening displacement (CMOD) to be evaluated.

$$CMOD = V_1 - \frac{h_1}{h_2 - h_1}(V_2 - V_1) \quad (5)$$

2.5. Unloading Compliance

The unloading compliance method assumes a monotonically increasing relation between crack depth and compliance. To evaluate the specimen's compliance during the test, it is partially unloaded and reloaded at predefined intervals of CMOD, as described in section 2.2. The slope of a linear regression line through the unloading data is then defined as the compliance. The required tensile force is obtained from the load cell of the test rig, the CMOD is obtained from the double clip gauge readings as described above in section 2.4.

Unfortunately, the compliance not only depends on the crack depth in SENT testing. Due to rotation of the specimen in combination with plasticity effects, the experimentally measured compliance do not necessarily increase monotonically. These effects were previously investigated and described by Verstraete et al. [15]. In accordance to this paper, an evaluation procedure was developed to evaluate

the crack extension based on finite element simulations and experimental observations. This procedure considers the compliances from initiation onwards. Crack initiation can thereby be identified by either of the following observations [31]:

- If the compliance curve shows a minimum, discard all compliance data prior to this minimum in the experimentally measured compliance curve. The point of minimum compliance represents crack initiation.
- If the compliance curve does not show a minimum, it most likely shows a linear increase of the compliance from the start of the test onwards. In this case, crack initiation is identified as the point where the compliance deviates from this linear trend. All compliance data prior to this deviation can be discarded.

The remaining compliances are subsequently translated into crack lengths using linear elastic compliance equations available in literature, as described in Appendix A [32]. However, as the proposed method discards all data prior to crack initiation, crack tip blunting is not accounted for. As a result, the crack extension attributed to blunting is explicitly added, based on the CTOD at initiation ($CTOD_{ini}$).

$$\begin{aligned} \Delta a_b &= CTOD/2 && CTOD \leq CTOD_{ini} \\ \Delta a_b &= CTOD_{ini}/2 && CTOD \geq CTOD_{ini} \end{aligned} \tag{6}$$

The predicted total crack extension using the unloading compliance technique ($\Delta a_{t,uc}$) therefore equals the sum of the crack extension predicted by the UC method (Δa_{uc}) and the crack extension attributed to crack tip blunting.

$$\Delta a_{t,uc} = \Delta a_{b,uc} + \Delta a_{uc} \tag{7}$$

Note that, since the point of initiation is determined from the unloading compliance data as discussed above, the blunting correction is denoted $\Delta a_{b,uc}$ in Eq. (7).

2.6. Direct Current Potential Drop

Analogous to the UC method, the DCPD method assumes a monotonically increasing relation between the potential drop across the crack ligament and the crack depth. To this end, a direct current of 25 A is remotely applied (Figure 3). This is sufficiently far away from the cracked ligament (four times the thickness of the specimen) to obtain a uniform current distribution [31]. To eliminate possible detrimental effects of current leakage, temperature changes and current changes on the measured potential drop across the crack, the two probe technique is adopted [16]. A first reference probe measurement (V_{ref}) is performed at a distance $2W$ from the cracked ligament. A second probe measures the potential drop across the crack (V). In practice, these measurement probes are connected to the bolts used to attach the knife blocks (section 2.4).

Both potential drop measurements are performed prior to each unloading cycle. The normalized potential drop, V/V_{ref}, is however not only affected by crack extension but also by the plastic deformation around the crack tip [33]. This undesirable effect is corrected for by subtracting a linear blunting line from the normalized signal (Figure 4). This blunting line is determined from a least squares fit using all measurement points in the linear region of the CMOD - V/V_{ref} graph. This approach has been well validated in the past [14,30]. The resulting signal is subsequently normalized by its initial value ($V_0/V_{ref;0}$). Following, the corresponding crack length is determined by means of the implicit form of Johnson's equation [34].

$$\frac{V(a)}{V(a_0)} = \frac{\cosh^{-1}\left(\frac{\cosh(9\pi/4W)}{\cos(\pi a/2W)}\right)}{\cosh^{-1}\left(\frac{\cosh(9\pi/4W)}{\cos(\pi a_0/2W)}\right)} \tag{8}$$

Analogous to the unloading compliance method, the potential drop method only considers the ductile crack extension after initiation. As a result, the predicted total amount of ductile crack extension (Δa_t) consists of both the crack extension predicted by the PD method (Δa_{pd}) and the crack extension attributed to crack tip blunting (Δa_b), Eq. (6).

$$\Delta a_{t,pd} = \Delta a_{b,pd} + \Delta a_{pd} \tag{9}$$

2.7. Evaluation method

To evaluate the accuracy of both the unloading compliance and the potential drop method, the calculated ductile crack extension is compared to the measured one. To that extent, after completion of the test, the specimens are first heat tinted at 200°C for 2 to 3 hours leading to oxidation of the fractured surface. Subsequently, the specimens are broken up in a brittle way after cooling the specimens in liquid nitrogen (Figure 5). The final crack extension is then determined using the nine points average method, as suggested by ASTM E1820 for SENB testing [9].

To analyze the accuracy, the standard deviation (*STD*) is calculated for all *N* tests listed in Table 1 and 2, via the following formula:

$$STD = \sqrt{\frac{1}{N}\sum_{i=1}^{N}\left(\Delta a_{9p,i} - \Delta a_{t,uc/pd,i}\right)^2} \tag{10}$$

Based on this calculated standard deviation, and furthermore assuming a normal error distribution, a 95% confidence interval is determined as ±1.96 STD. This allows evaluating the accuracy of the considered method as follows:

$$\Delta a_{t,uc/pd} = \Delta a_{9p} \pm 1.96 STD \tag{11}$$

3. Results

3.1. Accuracy

In general, Figure 6 indicates an excellent correspondence between the measured and calculated crack extension for both methods. This results in an overall accuracy of ± 0.34 mm (± 13%) and ± 0.31 mm (± 12%) for the unloading compliance and potential drop method respectively. This accuracy can be compared to the requirements in the ASTM E1820 standard for SENB testing [9]. It is stated that the difference should be limited to 15% of the average measured crack extension. This requirement is met for the current set of tests, whose relative difference did not exceed 11%.

In addition, in an attempt to evaluate the effectiveness of the presented method, the effect of the blunting correction has also been omitted from the analysis. On average, the predicted ductile crack extension is thereby underestimating the actual crack extension as measured using the nine points average method by 0.40 mm and 0.36 mm for the unloading compliance and potential drop method respectively (see also Figure 7).

3.2. Factors affecting the accuracy

Several factors are expected to influence the aforementioned accuracy. In the remainder of this section, the following factors are discussed:

- Presence of natural weld metal defects
- Initial crack size
- Crack front straightness

First, the focus is on the presence of natural weld metal defects. By means of example the measured and calculated ductile crack extension are compared for the welded SENT tests numbered WP2-xx and WP3-xx. These tests result in data points that are located close to or below the lower bound of the 95% confidence interval obtained using all test data (section 3.1 - indicated by the dotted lines in Figure 6). This observation is attributed to the presence of natural weld metal defects. In Figure 8, the fracture surface for specimen WP2-03 is shown. Multiple natural defects can easily be observed (white arrow signs). These natural defects contribute to the crack extension as measured by the nine points average method, though do not increase the potential drop across the crack during the test. The same applies for the unloading compliance method: the natural defects already decreased the initial compliance and are therefore not accounted for in the crack extension measurements during the test.

Given the absence of natural defects in base metal tests, a better correspondence is expected between the measured and calculated crack extension. This particularly holds for the potential drop method, where the data points are clearly contained within the 95% confidence interval. For the unloading compliance method (Figure 9), the results are somewhat biased since these base metal specimens have a wide range of relative crack depths. It has previously been shown that for specimens with a high initial crack depth the crack extension tends to be overestimated. In contrast, an underestimation is expected for shallow cracks [15]. This effect is indeed observed though the influence is clearly limited, indicating that the proposed method for the evaluation of the unloading compliance data performs satisfactorily.

A third factor that potentially influences the accuracy of the crack extension measurements, is the straightness of the crack front (e.g. tunneling) [21]. For the tests performed in the framework of this paper, an inverse tunneling is often observed; the crack grows more near the side grooves compared to the center of the specimen. This most likely indicates that the thickness reduction resulting from applying the side grooves is too high. To evaluate the influence of the crack front straightness, the parameter s_{cr} is introduced. This is calculated as the ratio of the standard deviation of the crack depths measured using the nine points average method (Δa_i) to the nine points averaged crack extension (Δa_{9p}).

$$s_{cr} = \sqrt{\frac{1}{9}\sum\left(\Delta a_i - \Delta a_{9p}\right)^2} \Big/ \Delta a_{9p} \tag{12}$$

In Figure 10.a these values are plotted against the relative error of the potential drop method for specimens WM-07 till WM-15. These specimens are selected since they are obtained from the same weld; though differ significantly in crack front straightness due to the different notching position (inner diameter vs. outer diameter vs. through thickness notch). A minor dependency on the crack front straightness is observed, though in general the influence of the crack front straightness is limited, particularly when realizing the extreme non-uniformity of some specimens involved in this series. For instance, the through-thickness notched specimen WM-15 (Figure 10.b) showed an extremely non-uniform crack extension pattern due to the heterogeneous nature of the sampled weld microstructures.

According to the ASTM E1820 requirements for SENB testing, such test result is not acceptable for evaluating the ductile tearing resistance. The aim of this paper is however to evaluate and compare the application limits of the crack growth measurement techniques. Hence, no attention has been paid to improve the validity of the test results, e.g. by pre-compressing the specimen to alleviate the residual stresses.

3.3. Crack initiation

Apart from the final crack extension, the CTOD-value corresponding to crack initiation ($CTOD_{ini}$) has also been compared for both methods. In Figure 11, the CTOD at initiation obtained from the potential drop method is plotted as function of the CTOD at initiation obtained using the unloading compliance method. Based on this data set, a linear regression analysis is performed. This revealed an excellent linear correlation ($R^2 = 0.9811$, close to 1). Furthermore, the obtained correlation almost perfectly demonstrates a 1-to-1 relationship (regression line slope 0.9753).

3.4. Impact on resistance curves

The tested materials, in particular the weld metals, are not homogeneous by nature. As a result, the obtained tearing resistance is expected to vary between geometrically identical test specimens (i.e. identical notch position and initial crack size) extracted from the same material. To capture this effect, the ASTM E1820 procedure requires at least three valid test results for each region of interest [9]. Accordingly, three SENT tests have typically been executed for each region of interest (with identical notch depth, orientation, …), grouped in a so-called configuration. These specimens have been extracted adjacent to each other.

For each configuration, the UC and DCPD data are considered for the evaluation of the ductile crack extension. For each crack growth measurement method and for each configuration, a curve fit is made based on all data points that are located between the 0.15 mm and 1.50 mm offset lines as illustrated in Figure 12.a. These lines are parallel to the blunting line, with an offset on the crack extension (Δa). In accordance to the ASTM E1820 standard, an exponential curve with two fitting parameters (δ_1 and δ_2) is constructed.

$$CTOD = \delta_1 (\Delta a)^{\delta_2} \tag{13}$$

In combination with this curve fit, a scatter band is calculated (Figure 12.b). The constant width of this scatter band δ_s is chosen to include 95% of all data points within a configuration; δ_s is regarded as a characteristic for the scatter and/or accuracy of the measured tearing resistance. The boundaries of the resistance curve can thus be written as:

$$CTOD = \delta_1 (\Delta a)^{\delta_2} \pm \delta_s \tag{14}$$

The scatter of the measured tearing resistance is evaluated for all configurations described in Table 1 and 2. It is concluded that both methods result in a similar scatter. On average, δ_s equals 0.15 mm for the potential drop method and 0.16 mm for the unloading compliance method. It might be argued that base metal specimens are more homogeneous and hence less prone to material property scatter. However, the scatter for these tests was not observed to differ considerably (0.20 mm on average) from that observed in the tests on welded specimens (0.14 mm on average).

4. Discussion

The main aim of this study was to compare both measurement techniques that allow for single specimen fracture toughness testing of R-curves in SENT specimens. A comparison of both methods is presented, taking into account aspects related to testing practice and result accuracy.

From a technical perspective, the results presented in the previous section do not identify any clear distinction between both techniques as both are similarly accurate. In the specific case of weld metal testing, the unloading compliance technique appeared slightly less susceptible to weld metal defects. On the other hand, the accuracy of the unloading compliance technique proved to be slightly dependent on the relative crack depth in contrast to the potential drop technique.

The successful interpretation of both measurement signals requires the determination of the point of crack initiation. An excellent correspondence was observed between both techniques. This again supports the equivalence of both measurement methods and adds belief to the validity of the proposed methods. It should however been noted that the determination of the point of crack initiation remains a most delicate question, requiring an experienced eye in case of both techniques. No analytical formula are available to strictly determine this initiation point. To that extent, it could be argued that one should eventually not necessarily select one of the presented techniques, though combine them. This will provide the fracture mechanics specialist confidence in the obtained test results.

A third technical aspect regards the scatter between specimens having an identical configuration (material region, notch depth, notch location and orientation, …). Regarding this aspect, the results obtained from both techniques did not show any relevant difference.

Whereas the technical arguments discussed in the previous paragraphs do not allow to differentiate between both techniques, there are some practical aspects which should be taken into account when selecting either of both techniques. With respect to the required test equipment, it is clear that the potential drop technique requires an additional investment for the current power source and precision voltage measurement apparatus. In contrast, two high precision clip gauges are required for the unloading compliance technique. This accuracy would probably not be required if these clip gauges were used solely to determine the CTOD and/or CMOD, as would be the case for the potential drop technique. It is expected that the cost for these clip gauges is smaller compared to the potential drop equipment, thus requiring a higher initial investment for the potential drop method. On the other hand, the time needed for testing one specimen is theoretically shorter for the potential drop technique, as it does not require the time-consuming unloading cycles. The presented results also demonstrated that there is no need for insulation of the test specimens when using the potential drop method including a reference voltage measurement. Although insulation might be achievable for smaller specimens, this is definitely an asset when considering the evaluation of ductile crack extension in large scale specimens (e.g. curved wide plate specimens [35]).

5. Conclusion

To allow the evaluation of the fracture toughness by using SENT testing, two single specimen methods have been presented and compared, namely the unloading compliance and direct current potential drop technique. Based on an extensive set of experimental data, it has been demonstrated that these techniques are equivalent from a performance point of view; no differences in accuracy, scatter or moment of initiation have been observed. From a practical perspective, however, one should take into account the differences between both techniques, for instance the required time for performing one test and the required investments.

6. Acknowledgements

The authors would like to acknowledge the financial support of the IWT (Agency for Innovation by Science and Technology – Grant Nos. SB-091512 and SB-093512) and the FWO (Research Foundation Flanders – Grant Nos. 1.1.880.09.N.00 and 1.1.880.11.N.01). Finally, Dr. W.R. Tyson and Dr. G. Wilkowski are acknowledged for the numerous fruitful discussions and sharing their experiences.

7. Appendix A: Unloading Compliance Equations

To convert the measured compliances to actual crack sizes, elastic-plastic finite element simulations can be considered [15]. Given their complexity, preference has been given in this paper to a more hands-on, analytical approach. A number of equations are available in literature, all based on elastic 2D finite element simulations [12,13,36,37]. A comparative study indicated only minor differences between these equations. Therefore, the formulation proposed by Shen et al. is considered in this paper [13].

This approach starts from a generalized m-th degree relation between the compliance and the relative crack depth (a/W).

$$\frac{a}{W} = \sum_{i=0}^{m} r_i U^i \tag{A.1}$$

In the above equation, U is calculated from the specimen's effective thickness (B_e), compliance (C) and Young's modulus (E).

$$U = \frac{1}{1+\sqrt{B_e C E}} \tag{A.2}$$

Shen et al. determined the coefficients r_i in Eq. A.1. from 2D plane strain finite element simulations of SENT specimens with a relative crack depth ranging between 0.05 and 0.95. These curve fitting parameters are listed in Table A.1 (m = 8).

8. References

[1] Wang, Y. Y., Liu, M., Zhang, F., Horsley, D., and Nanney, S., 2012, "Multi-Tier Tensile Strain Models for Strain-Based Design - Part 1: Fundamental Basis", International Pipeline Conference, Calgary, Alberta, Canada, paper n° IPC2012-90690.

[2] Fairchild, D. P., Macia, M. L., Kibey, S., Wang, X., Krishnan, V. R., Bardi, F., Tang, H., and Cheng, W., 2011, "A Multi-Tiered Procedure for Engineering Critical Assessment of Strain-Based Pipelines", International Offshore and Polar Engineering Conference, Maui, HI, United States, pp. 698-705.

[3] Cravero, S., Bravo, R. E., and Ernst, H. A., 2008, "Constraint Evaluation and Effects on J-R Resistancecurves for Pipes under Combined Load Conditions", International Offshore and Polar Engineering Conference, Vancouver, British Columbia, Canada, pp. 149-156

[4] Xu, J., Zhang, Z. L., Ostby, E., Nyhus, B., and Sun, D. B., 2010, "Constraint Effect on the Ductile Crack Growth Resistance of Circumferentially Cracked Pipes", Engineering Fracture Mechanics, 77, pp. 671-684.

[5] Cravero, S., and Ruggieri, C., 2004, "Integrity Assessment of Pipelines Using SE(T) Specimens", International Pipeline Conference, Calgary, Alberta, Canada, paper n° IPC04-0033.

[6] Det Norske Veritas, 2006, RP-F108: Fracture Control for Pipeline Installation Methods Introducing Cyclic Plastic Strain.

[7] Zhou, D. W., 2011, "Measurement and Modelling of R-Curves for Low- Constraint Specimens", Engineering Fracture Mechanics, 78, pp. 605-622.

[8] Pussegoda, L. N., Tiku, S., Park, D.-Y., Tyson, W. R., and Gianetto, J. A., 2012, "J-Resistance Results from Multi-Specimen and Single-Specimen Surface Notched SEN(T) Geometry", International Pipeline Conference, Calgary, Alberta, Canada, paper n° IPC2012-90565.
[9] American Society of Testing and Materials, 2011, E1820 - Standard Test Method for Measurement of Fracture Toughness.
[10] British Standard, 2013, BS7910 - Guide to methods for assessing the acceptability of flaws in metallic structures, in Annex N - Allowance for constraint effects.
[11] Moore, P. L., and Pisarski, H. G., 2012, "Validation of Methods to Determine CTOD from SENT Specimens", International Offshore and Polar Engineering Conference, Rhodes, Greece, pp. 577-582.
[12] ExxonMobil, 2010, "Measurement of Crack Tip Opening Displacement (CTOD) - Fracture Resistance Curves Using Single-Edge Notched Tension (SENT) Specimens," ExxonMobil Upstream Research Company, Houston.
[13] Shen, G., Gianetto, J. A., and Tyson, W. R., 2009, "Measurement of J-R Curves Using Single Specimen Technique on Clamped SE(T) Specimens", International Offshore and Polar Engineering Conference, Osaka, Japan, pp. 92-99.
[14] Wilkowski, G., Shim, D. J., Kalyanam, S., Wall, G., Mincer, P., Rider, D., Brust, F. W., and Rudland, D. L., 2009, "Using D-C Electric Potential for Crack Initiation/Growth Monitoring During Testing of Weld Metal Fracture Specimens", Pipeline Technology Conference, Ostend, Belgium, paper n° Ostend2009-018.
[15] Verstraete, M.A., Hertelé, S., Denys, R.M., Van Minnebruggen, K., De Waele, W., 2014, “Evaluation and interpretation of ductile crack extension in SENT specimens using unloading compliance technique”, Engineering Fracture Mechanics, 115, pp. 190-203.
[16] Verstraete, M.A., Denys, R.M., Van Minnebruggen, K., Hertelé, S., De Waele, W., 2013, “Determination of CTOD resistance curves in side-grooved Single-Edge Notched Tensile specimens using full field deformation measurements”, Engineering Fracture Mechanics, 110, pp. 12-22.
[17] British Standard, 2014, BS8571 - Method of test for determination of fracture toughness in metallic materials using single edge notched tension (SENT) specimens.
[18] Det Norske Veritas, 2012, OS-F101: Submarine Pipeline Systems.
[19] Akourri, O., Louah, M., Kifani, A., Gilgert, G., and Pluvinage, G., 2000, "The Effect of Notch Radius on Fracture Toughness J(Ic)", Engineering Fracture Mechanics, 65, pp. 491-505.
[20] Lan, W., Deng, X., and Sutton, M. A., 2010, "Investigation of Crack Tunneling in Ductile Materials", Engineering Fracture Mechanics, 77, pp. 2800-2812.
[21] Riemelmoser, F. O., Pippan, R., Weinhandl, H., and Kolednik, O., 1999, "The Influence of Irregularities in the Crack Shape on the Crack Extension Measurement by Means of the Direct-Current-Potential-Drop Method", Journal of Testing and Evaluation, 27, pp. 42-46.
[22] Shen, G., Tyson, W. R., Gianetto, J. A., and Park, D.-Y., 2010, "Effect of Side Grooves on Compliance, J-Integral and Constraint of Clamped SE(T) Specimen", Pressure Vessels and Piping Conference, Bellevue, Washington, USA, paper n° PVP2010-25164.
[23] CANMET, 2010, "Recommended Practice: Fracture Toughness Testing Using SE(T) Samples with Fixed-Grip Loading," CANMET Materials Technology Laboratory, Ottawa.
[24] Hertelé, S., De Waele, W., Denys, R, Verstraete, M.A., Van Minnebruggen, K. and Horn, A., 2013, "Weld Strength Mismatch in Strain Based Flaw Assessment: Which Definition to Use?", Journal of Pressure Vessel Technology-Transactions of the ASME, 135, pp. 1-8.
[25] Tang, H., Minnaar, K., Kibey, S., Macia, M. L., Gioielli, P., and Fairchild, D. P., 2010, "Development of the SENT Test for Strain-Based Design of Welded Pipelines", International Pipeline Conference, Calgary, Alberta, Canada, paper n° IPC2010-31590.

[26] Fagerholt, E., Ostby, E., Borvik, T., and Hopperstad, O. S., 2012, "Investigation of Fracture in Small-Scale SENT Tests of a Welded X80 Pipeline Steel Using Digital Image Correlation with Node Splitting", Engineering Fracture Mechanics, 96, pp. 276-293.

[27] Cicero, S., Gutiérrez-Solana, F. and Álvarez, J. A., 2008, "Structural Integrity Assessment of Components Subjected to Low Constraint Conditions", Engineering Fracture Mechanics, 75, pp. 3038-3059.

[28] Rice, J. R., 1968, "A Path Independent Integral and the Approximate Analysis of Strain Concentration by Notches and Cracks", Journal of Applied Mechanics, 35, pp. 379-386.

[29] Verstraete, M.A., Denys, R.M., Van Minnebruggen, K., Hertelé, S., De Waele, W., 2013, "Determinations of CTOD resistance curves in side-grooved Single-Edge Notched Tensile specimens using full field deformation measurements", Engineering Fracture Mechanics, 110, pp. 12-22.

[30] Manzione, P., and Perez Ipiña, J., 1991, "Sensitivity Analysis of the Double Clip Gauge Method", Fatigue and Fracture Of Engineering Materials and Structures, 14, pp. 887-869.

[31] Verstraete M.A., "Experimental-Numerical Evaluation of Ductile Tearing Resistance and Tensile Strain Capacity of Biaxially Loaded Pipelines", PhD thesis, Ghent University, 2013.

[32] Shen, G., and Tyson, W. R., 2009, "Crack Size Evaluation Using Unloading Compliance in Single-Specimen Single-Edge-Notched Tension Fracture Toughness Testing", Journal of Testing and Evaluation, 37, pp. 347-357.

[33] Chipperfield, C. G., 1976, "Detection and Toughness Characterisation of Ductile Crack Initiation in 316 Stainless Steel", International Journal of Fracture, 12, pp. 873-886.

[34] Johnson, H. H., 1965, "Calibrating the Electric Potential Method for Studying Slow Crack Growth", Materials Research and Standards, pp. 442-445.

[35] Hertelé, S., De Waele, W., Denys, R.M., Verstraete, M.A., 2012, "Investigation of Strain Measurements in (Curved) Wide Plate Specimens Using Digital Image Correlation and Finite Element Analysis", Journal of Strain Analysis for Engineering Design, 47(5), pp. 276-288.

[36] Cravero, S., Ruggieri, C., 2007, "Estimation procedure of J-resistance curves for SE(T) fracture specimens using unloading compliance", Engineering Fracture Mechanics, 74, p. 2735-2757.

[37] Fonzo, A., Melis, G., Di Vito, G., Mannucci, G., Darcis, P, Richard, G., Quintanilla, H., Armengol, M., 2009, "Measurement of fracture resistance of pipelines for strain based design", 17th Biennial Joint Technical Meeting on Pipeline Research, Milan, Italy. p. 1-8.

Figures

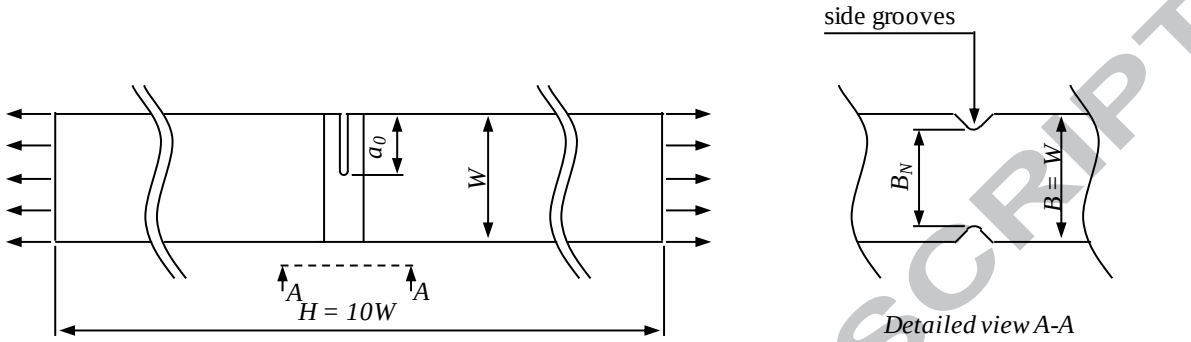

Figure 1 – Geometry of test specimens

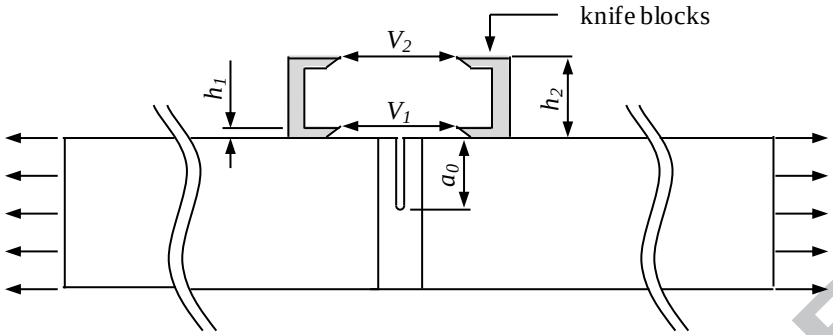

Figure 2 – Illustration of mounting pieces attached to a SENT specimen, allowing to measure CTOD via double clip gauge method

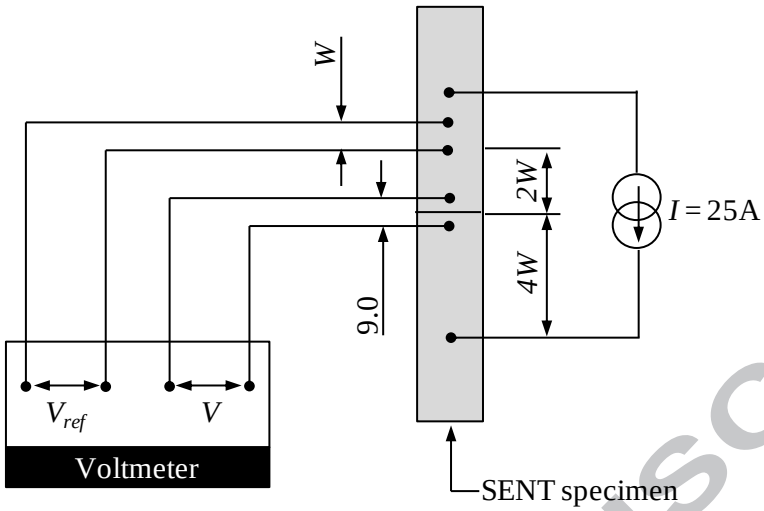

Figure 3 – Schematic representation of current in- and output pins
and measurement probes for potential drop measurements in SENT specimens

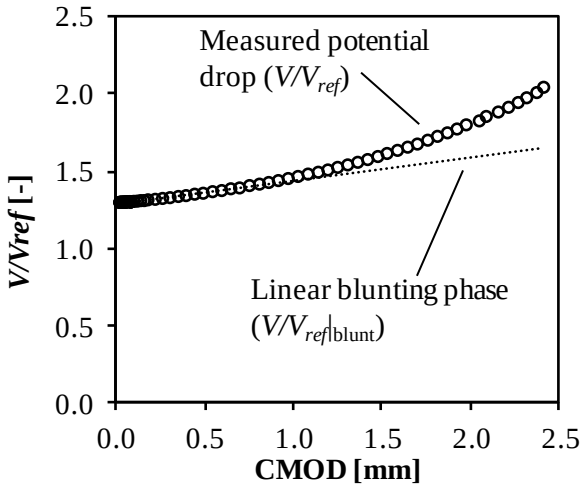

Figure 4 – Illustration of linear blunting phase obtained from potential drop measurements

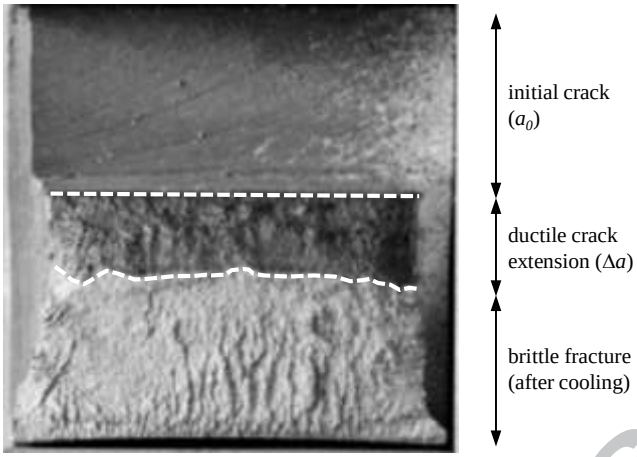

Figure 5 – Example fracture surface after heat tinting for specimen WM-03

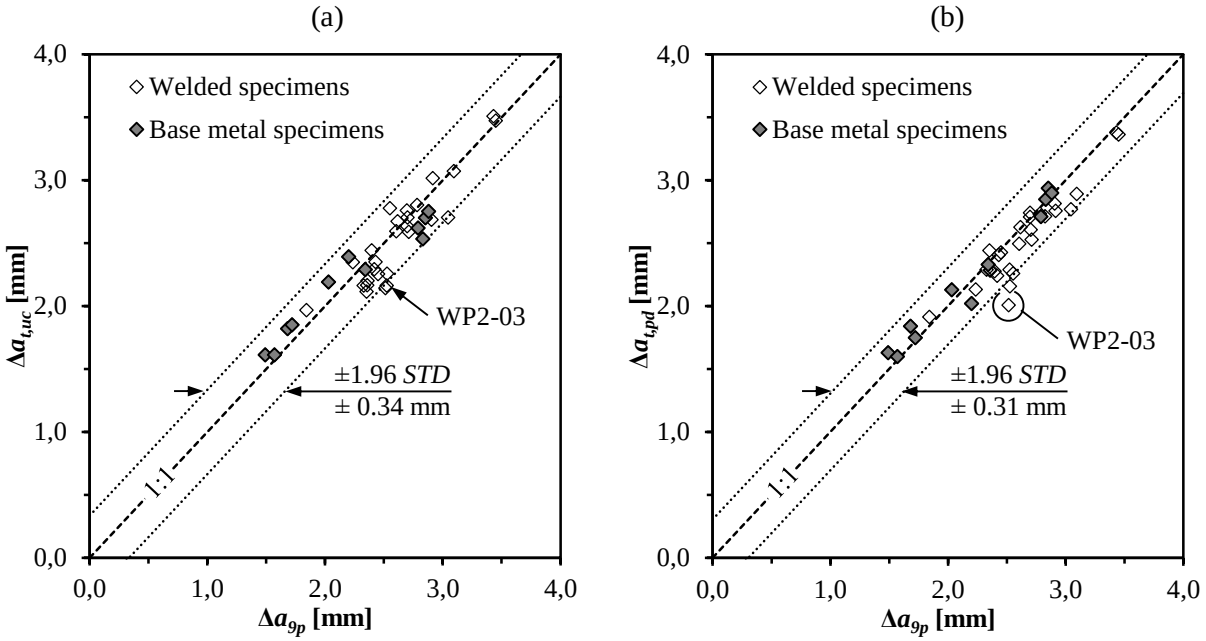

Figure 6 - Evaluation of accuracy for unloading compliance (a) and direct current potential drop (b) method during SENT testing

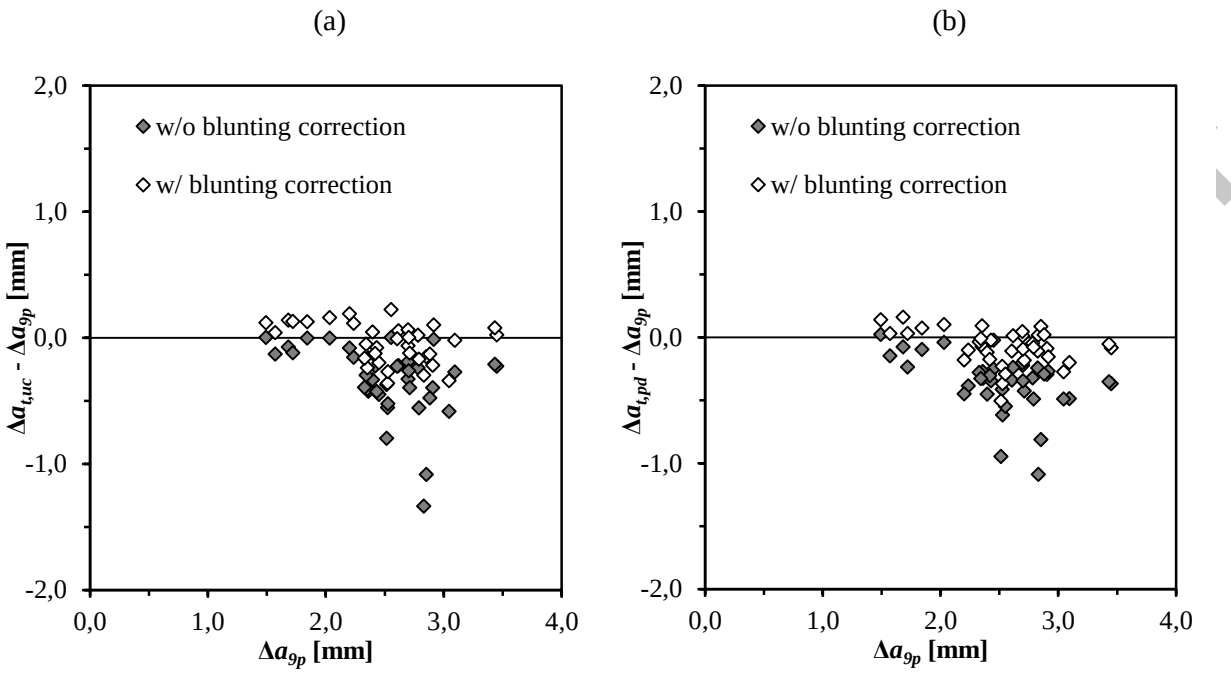

Figure 7 – Effect of blunting correction on the accuracy of the predicted crack extensions for the unloading compliance (a) and direct current potential drop (b) method

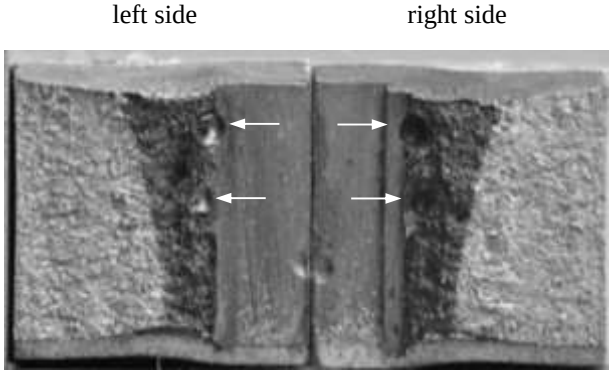

Figure 8 – Fracture surface for specimen WP2-03 clearly showing the presence of natural weld defects in the zone of ductile crack extension (indicated by white arrow signs)

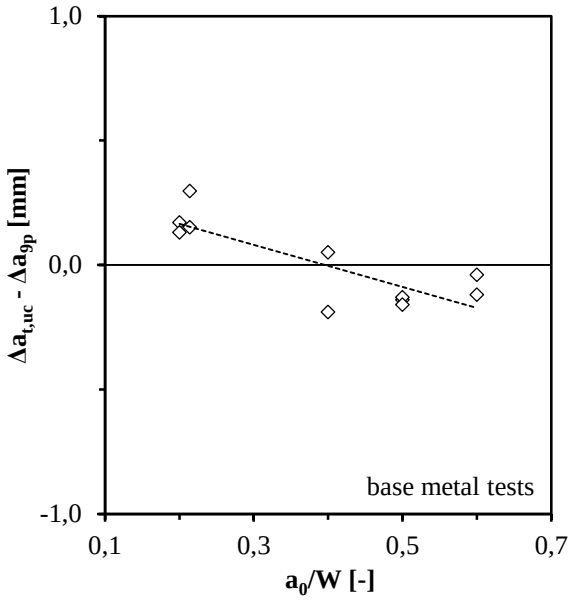

Figure 9 – Evaluation of accuracy for unloading compliance method for homogeneous base metal SENT tests

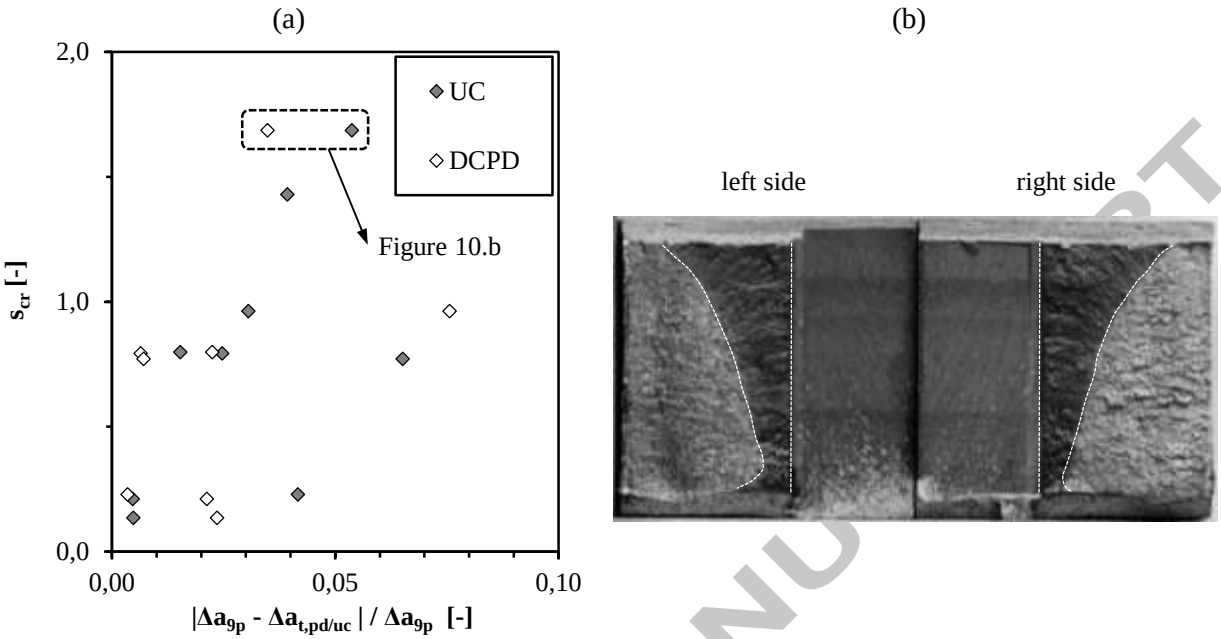

Figure 10 – Influence of crack front straightness on accuracy of predicted crack extension for potential drop method for specimens WM-07 to WM-15 (a) and fracture surface showing highly non-uniform crack extension for specimen WM-15 with a notch located in the through-thickness direction (b)

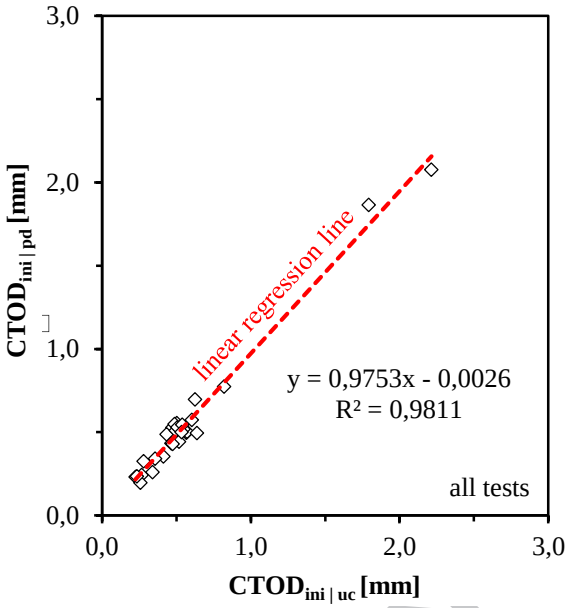

Figure 11 - Predicted CTOD corresponding to crack initiation for unloading compliance method versus potential drop method

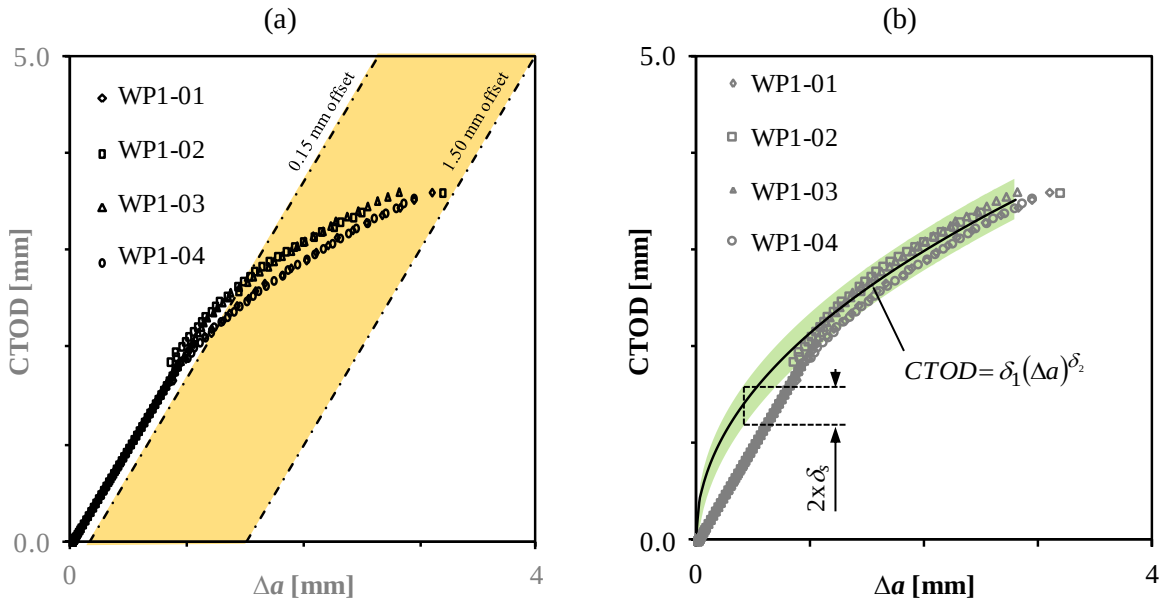

Figure 12 - Data points considered to determine tearing resistance curve (a) and fitted curve in combination with scatter band (b)

Tables

Table 1 – Overview of homogeneous (i.e. non-welded) SENT specimens

Specimen	B [mm]	W [mm]	a_0 / W [-]	API-5L Grade	Y / T [-]
BM-01	15.0	15.0	0.20	X80	0.86
BM-02	15.0	15.0	0.20	X80	0.86
BM-03	15.0	15.0	0.40	X80	0.86
BM-04	15.0	15.0	0.40	X80	0.86
BM-05	15.0	15.0	0.60	X80	0.86
BM-06	15.0	15.0	0.60	X80	0.86
BM-07	15.0	15.0	0.50	X80	0.86
BM-08	15.0	15.0	0.50	X80	0.86
BM-09	15.0	15.0	0.50	X80	0.86
WP1-01	14.0	14.0	0.21	X65	0.82
WP1-02	14.0	14.0	0.21	X65	0.82
WP1-03	14.0	14.0	0.21	X65	0.82
WP1-04	14.0	14.0	0.21	X65	0.82

Table 2 – Overview of welded SENT specimens

Specimen	$W = B$ [mm]	a_0/W [-]	API-5L Grade	Y/T_{BM} [-]	Y/T_{WM} [-]	Notch	Welding Process	MM_{FS} [%]
WM-01 WM-02 WM-03	12.5	0.50	X80	0.91	0.83	WMC root	SMAW	+1
WM-04 WM-05 WM-06	12.5	0.50	X80	0.91	0.93	WMC root	GMAW	+33
WM-07 WM-08 WM-09	15.0	0.40	X80	0.86	0.93	WMC cap	GMAW	+20
WM-10 WM-11 WM-12	15.0	0.40	X80	0.86	0.93	WMC root	GMAW	+20
WM-13 WM-14 WM-15	15.0	0.40	X80	0.86	0.93	WMC through thickness	GMAW	+20
WP2-01 WP2-02 WP2-03 WP2-04 WP2-05 WP2-06	11.5	0.28	X70	0.90	0.91	WMC root	GMAW	+6
WP3-01 WP3-02 WP3-03 WP3-04 WP3-05	11.5	0.28	X70	0.92	0.89	WMC root	GMAW	+0
WP4-01 WP4-02 WP4-03	14.0	0.30	X80	0.89	0.94	WMC root	GMAW	+8
WP5-01 WP5-02 WP5-03	14.0	0.30	X80	0.91	0.94	WMC root	GMAW	+0

Table A.1. Curve fitting constants for parameters in Eq. A.1 [13]

r_0	r_1	r_2	r_3	r_4	r_5	r_6	r_7	r_8
2.072	-16.411	-79.600	-211.670	236.857	27.371	-179.740	-86.280	171.764

Nomenclature

a	crack depth
a_0	initial crack depth
B	thickness
B_e	effective thickness
B_N	net thickness
CMOD	Crack Mouth Opening Displacement
CTOD	Crack Tip Opening Displacement
$CTOD_{ini}$	CTOD at initiation
DCPD	Direct Current Potential Drop
F_{max}	maximum force
h_1	height of first clip gauge above specimen
h_2	height of second clip gauge above specimen
H	daylight grip length
I	applied current (25 A for all tests)
MM_{FS}	mismatch in terms of flow stress
N	batch size
P_m	limit load
s_{cr}	crack front straightness parameter
SENT	Single-Edge Notched Tensile
STD	standard deviation
V	potential drop across the crack
V_1	opening of first clip gauge
V_2	opening of second clip gauge
UC	Unloading Compliance
V_{ref}	potential drop remote from the crack
W	width
WMC	Weld Metal Center
Y/T	Yield-to-Tensile ratio
δ_1	curve fitting parameter for R-curve
δ_2	curve fitting parameter for R-curve
Δa	crack extension
$\Delta a_{b,uc/pd}$	crack extension attributed to blunting for unloading compliance and potential drop method
Δa_{9p}	measured crack extension using nine points average method
δ_s	width of scatter band in terms CTOD
σ_0	yield strength
σ_{FS}	flow strength
σ_{TS}	tensile strength

Highlights

- DCPD en UC suitable for evaluation of ductile crack extension in SENT specimens
- Crack front straightness does not affect accuracy of crack extension measurements
- No difference in accuracy and moment of initiation between both methods